

FRACTURE TOUGHNESS OF TURBINE ROTOR SHAFT  
AND VALIDITY CRITERION FOR  $K_{IC}$

K. Ikeda\* M. Aoki\* H. Kikuchi\*\*  
U. Schieferstein\*\*\* and C. Berger\*\*\*

INTRODUCTION

According to the ASTM validity criteria for the plane strain fracture toughness,  $K_{IC}$ , the measured fracture toughness should satisfy the following conditions [1]: (i) the specimen geometry validity,  $a$  and  $B \geq 2.5 \times (K_Q/\sigma_y)^2$ , (ii) the load-displacement curve validity,  $P_{max} < 1.1 P_Q$ . The limited section of material taken from various components of structures often makes the thickness criterion a difficult one to meet. In this paper, very large disc type specimens of 345 mm thick and 920 mm dia. prepared from low-pressure turbine rotor shafts were tested to evaluate the valid fracture toughness.

In addition, the validity criterion for  $K_{IC}$  has been investigated by using various sizes of compact tension specimens, and proposed as  $P_{max} = P_Q$ .

MATERIALS AND TESTING PROCEDURES

The materials tested are 2.8Ni-Cr-Mo-V steels for low pressure turbine rotor and the three discs were prepared from prolonged parts of rotor shafts manufactured by Kobe Steel, Ltd. as shown in Figure 1. The chemical composition, quality heat treatment and mechanical properties of the three discs are presented in Tables 1 through 3. The two rotor and prolongation test forgings were heat treated as one solid piece each.

After the 14 RCT specimens (Round Compact Tension specimen of 14 inch thick) [2] shown in Figure 2, which had the original diameter of the prolonged forgings, were tested, various sizes of smaller CT specimens (Compact Tension specimen) were taken from the central and mid-thickness portions of the 14 RCT specimens.

To our best knowledge, the 14 RCT specimens used for this investigation are the largest fracture toughness specimens ever tested in this world. The smaller specimens were of the sizes 1, 3 and 6 CT/ASTM-E399 [1].

A fatigue testing machine of large load capacity is needed to precrack the tip of the machined chevron notch of 14 RCT specimen. Indeed, the fatigue precracking of 14 RCT specimen was carried out at the cyclic rate of 1 Hertz and the cyclic load of 0-1,500 kN which was produced by the combination of the  $\pm 600$  kN servo-hydraulic testing machine and the load-amplifying clevis shown in Figure 3, in which the principles of lever are utilized. The pins, D, in Figure 3 are located at both surfaces of

\*Structural Engineering Laboratory, Kobe Steel, Ltd., Japan.

\*\*Steel Casting & Forging Division, Kobe Steel, Ltd., Japan.

\*\*\*Materials Engineering and Research Division, Kraftwerk Union AG., Muelheim/Ruhr, West Germany.

the 14 RCT specimen and play a role of fulcrum subjected to compression. The supporting bed, S, whose surface has the larger radius of curvature than that of the 14 RCT specimen, may convert the horizontal displacement of RCT specimen due to loading into a rotational one with minimum friction. It takes about  $300 \times 10^3$  cycles to precrack by about 10 mm at the tip of a machined chevron notch on the surface of RCT specimen. The fracture tests of the precracked RCT specimen were conducted by using a 30,000 kN tensile testing machine.

The precracking and fracture testing of the smaller-sized CT specimens was conducted by using a  $\pm 600$  kN servo-hydraulic and a 3,000 kN tensile testing machine, respectively.

The load as a function of clip gage displacement at the edge of notch was plotted by using an X-Y recorder. The fatigue precracking and the measurement of the crack lengths after fracture were carried out according to ASTM-E399.

The measured fracture toughness,  $K_Q$ , is said to be a valid one,  $K_{IC}$ , if the following requirements are met:

$$a \text{ and } B \geq 2.5(K_Q/\sigma_Y)^2 \quad (1)$$

$$P_{\max} < 1.10 P_5 \quad (2)$$

where

- a: crack length,
- $\sigma_Y$ : yield stress,
- B: specimen thickness,
- $P_{\max}$ : fracture load,
- $P_5$ : load at which the secant drawn on the load-displacement record at a slope 5% less than that of the load-displacement curve at the origin, cuts. (see Figure 4)

In general, three different types of load-displacement curves are produced as shown in Figure 4. The requirement of equation (2) is met for the curves of Figures 4(a) and 4(b). The following requirement of equation (3) proposed in this paper which is more conservative than that of equation (2), is met only for the curve where  $P_{\max}$  occurred before  $P_5$  as shown in Figure 4(a), however, this does not necessarily guarantee geometric validity, equation (1).

$$P_{\max} = P_Q \quad (3)$$

The testing temperature of the smaller CT specimens taken from the fractured 14 RCT ones was determined so as to satisfy all the following three conditions independently of specimens A, B and C: (i) In case of 6 CT test, both the requirements of equations (1) and (3) are met. (ii) In case of 3 CT test, the requirement of equation (1) is not met but that of equation (3) is met. (iii) In case of 1 CT test, neither the requirement of equation (1) nor equation (3) is met.

## TEST RESULTS AND DISCUSSION

### CT test

The effects of specimen thickness on fracture toughness from various sizes of CT test specimen are shown in Figure 5. The thickness of CT specimen means the size of that. The load-displacement records are shown in Figure 6.  $K_Q$  value from 6 CT test is said to be a valid estimate of  $K_{IC}$ , because both the requirements of equations (1) and (3) are met.  $K_Q$  from 3 CT test does not satisfy equation (1) but equation (3), however, that value is found to be nearly equal to the  $K_{IC}$  value from the 6 CT test.  $K_Q$  from 1 CT satisfies neither equation (1) nor equation (3), and that value is always smaller than  $K_{IC}$  value.

Therefore, valid  $K_{IC}$ -values may well be measured even if the specimen geometry requirement, equation (1), is not fulfilled. The important point is that fracture occurs within the elastic region, that is, within the linear part of the load-displacement curve.

Then, it is concluded that "invalid" fracture toughness value,  $K_Q$ , can be regarded as a valid one,  $K_{IC}$ , as long as the requirement of equation (3) is met.  $K_{IC}^W$  in Figure 5 is the predicted  $K_{IC}$  value from "invalid" test by employing the equivalent energy method suggested by Witt and Mager [3] and  $K_{IC}^C$  by the application of the Bilby-Cottrell-Swinden model [4] to CT test as proposed by Chell et al. [5].

Where the linearity of load-displacement curve is approximately kept to the point of fracture as in the 3 CT test, the values of  $K_{IC}^W$  and  $K_{IC}^C$  are nearly equal to that of  $K_{IC}$ . However, where the requirement of equation (3) is not met as in the 1 CT test, the values of  $K_{IC}^W$  and  $K_{IC}^C$  are considerably different from that of  $K_{IC}$ .

### 14 RCT test

At first, the loading on specimen B of 14 RCT was carried out at 10°C. The load-displacement record is shown in Figure 7. Fracture did not occur after  $P_Q$  in Figure 7. Then, the fracture tests of specimens A and C of 14 RCT were conducted at -20°C and -30°C, respectively.  $K_Q$  from RCT test is calculated from the equation (2):

$$K_Q = P_Q / (B \cdot W) \cdot \sqrt{a} F(a/W) \quad (4)$$

$$F(a/W) = 29.6 - 162 (a/W) + 492.6 (a/W)^2 - 663.4 (a/W)^3 + 405.6 (a/W)^4 \quad (5)$$

where W is the specimen width.

$K_Q$  from specimen A does not satisfy the requirement for "a" of equation (1) but for "B". However, this  $K_Q$  value can be regarded as  $K_{IC}$ , because the requirement of equation (3) is met.  $K_Q$  from specimens B and C are not regarded as  $K_{IC}$ , because the requirement of equation (3) is not met. Material for specimen C shows higher toughness than that for specimens A and B.  $K_{IC}$  values obtained from 14 RCT, 6 CT and 3 CT tests are shown in Figure 8 as a function of temperature in comparing with available  $K_{IC}$ -data points from 2.8Ni-Cr-Mo-V rotor forgings [6,7]. For reference  $K_Q$  from the 14 RCT tests are also shown in this figure. It is noted in Figure 8

that the fracture toughness of forgings tested are at the upper bound of the scatterband established by the tests with specimens from other rotor forgings.

#### CONCLUSIONS

The invalid fracture toughness  $K_Q$  according to ASTM specification can be regarded as the valid one,  $K_{IC}$ , so long as the approximate linearity of load-displacement curve,  $P_{max}=P_Q$ , is kept to the point of fracture.

#### REFERENCES

1. ASTM Standard Designation E399-74, 960.
2. FEDDERN, G. and MACHERAUCH, E., Z. Metallkde., 64, 1973, 882.
3. WITT, F. J. and MAGER, T. R., Fifth National Symposium on Fracture Mechanics, University of Illinois, September 1971.
4. BILBY, B. A., COTTRELL, A. H. and SWINDEN, K. H., Proc. Roy. Soc., A272, 1963, 304.
5. CHELL, G. G., MILNE, I. and KIRBY, J. H., Metals Technology, 2, 1975, 549.
6. SCHINN, R., STAIF, F. and WIEMANN, W., VGB-Kraftwerkstechnik, 54, 1974, 456.
7. Kraftwerk Union AG., Muelheim/Ruhr, Germany, Unpublished company data.

Table 1 Chemical composition of test material

Specimen	Chemical Compositions, % <sup>1)</sup>												
	C	Si	Mn	P	S	Cr	Mo	Ni	V	As	Cu	Sb	Sn
A	0.27	0.07	0.32	0.007	0.009	1.49	0.34	2.86	0.08	0.003	0.02	0.0039	0.003
B													
C	0.28	0.03	0.29	0.008	0.009	1.66	0.35	2.94	0.10	0.002	0.02	0.0014	0.002

1) heat analysis, average value

Table 2 Quality heat treatment of test material

Specimen	Quality heat treatment
A + B	830°C 35h / water spray quench + 630°C 66h / controlled furnace cool
C	850°C 35h / water spray quench + 830°C 35h / water spray quench + 630°C 40h / controlled furnace cool

Table 3 Mechanical properties of test material

Specimen <sup>1)</sup>	$\sigma_{0.2}$ N/mm <sup>2</sup>	$\sigma_B$ N/mm <sup>2</sup>	Elong. %	R.A. %	Number of tests
A + B	629~679				14
		758~882	13~20	54~62	21
C	680~720				14
		802~861	17~21	58~64	16

1) Specimen orientation and distribution :  
radial over total cross-section of 920 mm dia-  
prolongation forging.

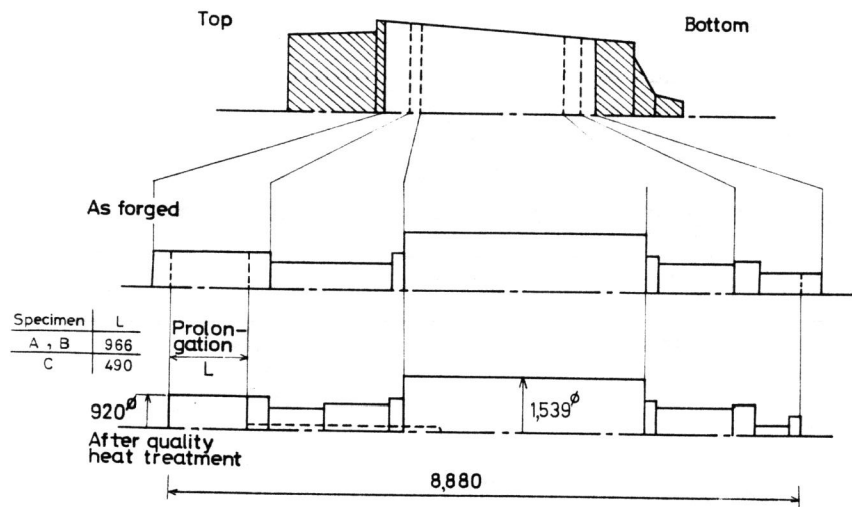


Figure 1 Relative position of rotor and prolongation test forging in the 150 ton ingot and the 85 ton forging

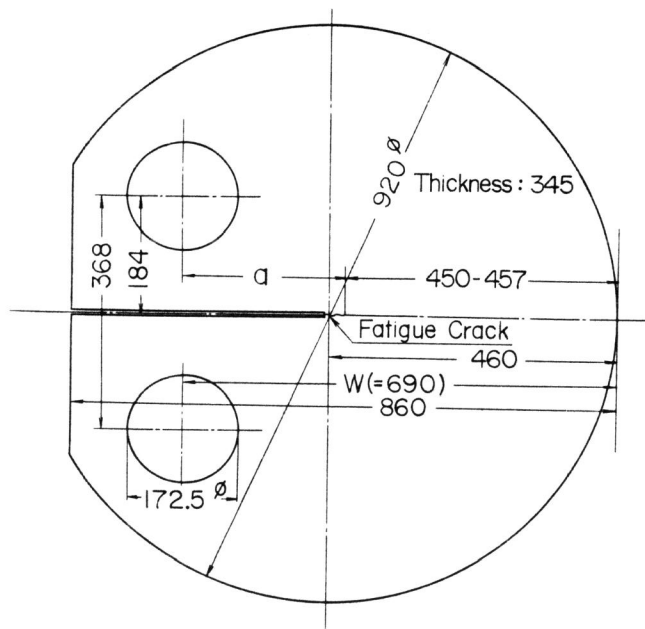


Figure 2 14 RCT specimen [2]

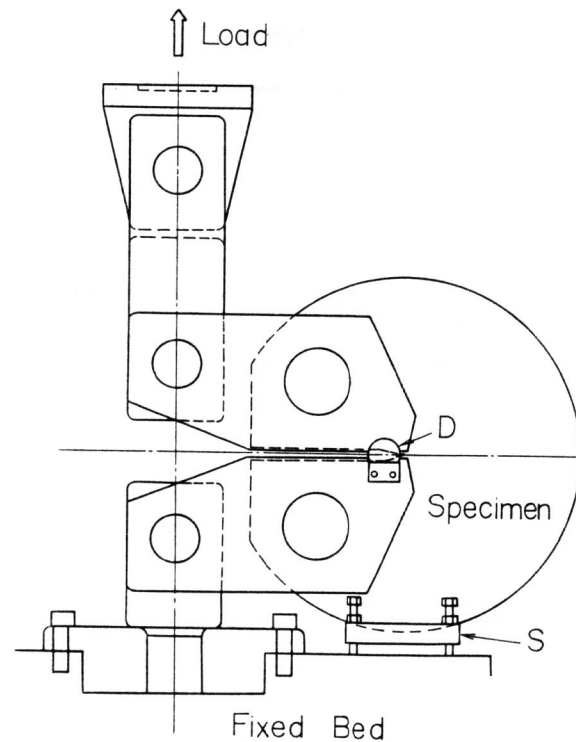


Figure 3 Clevis for fatigue cracking of 14 RCT specimen

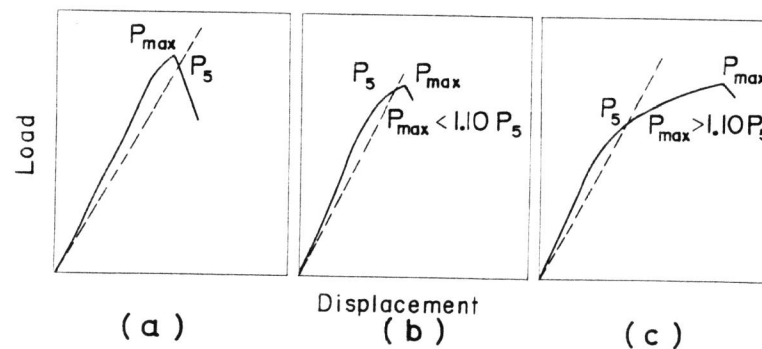


Figure 4 Three types of load-displacement record

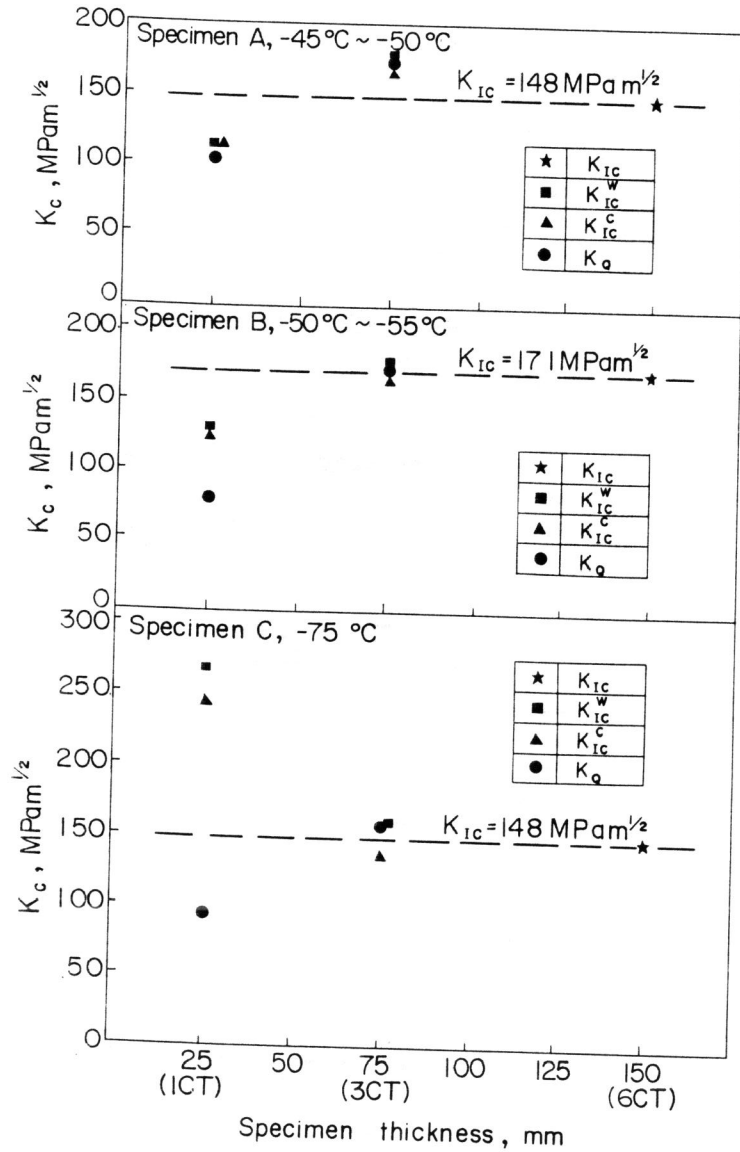


Figure 5 Effect of specimen size on fracture toughness value

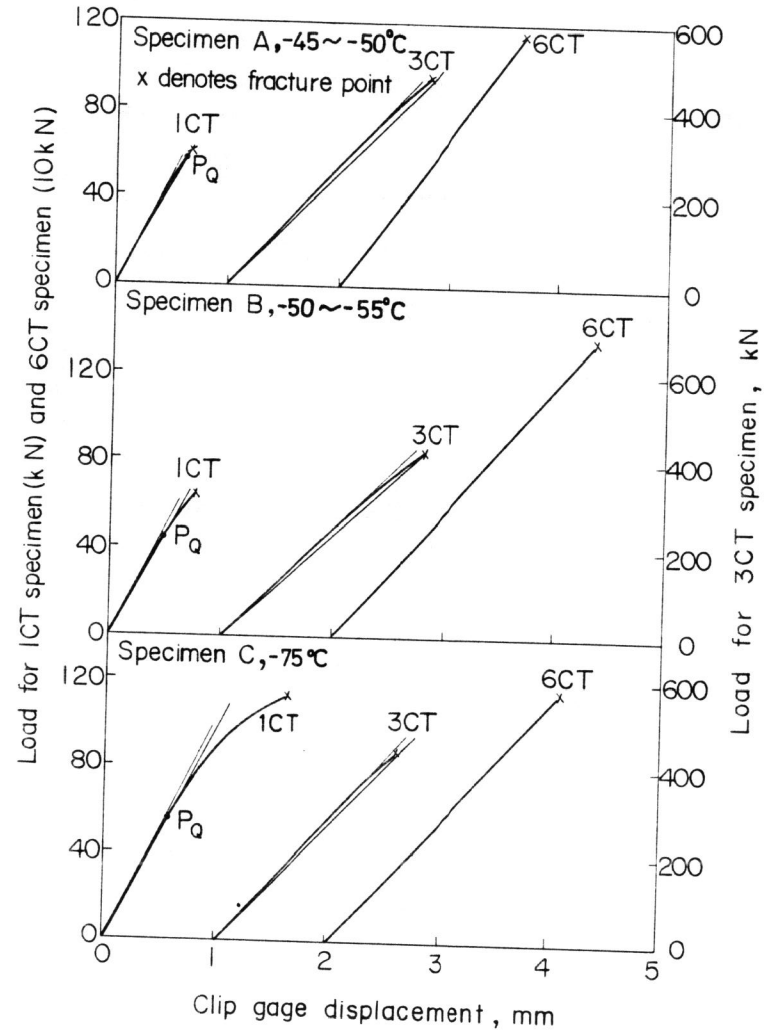


Figure 6 Load-displacement records of CT tests

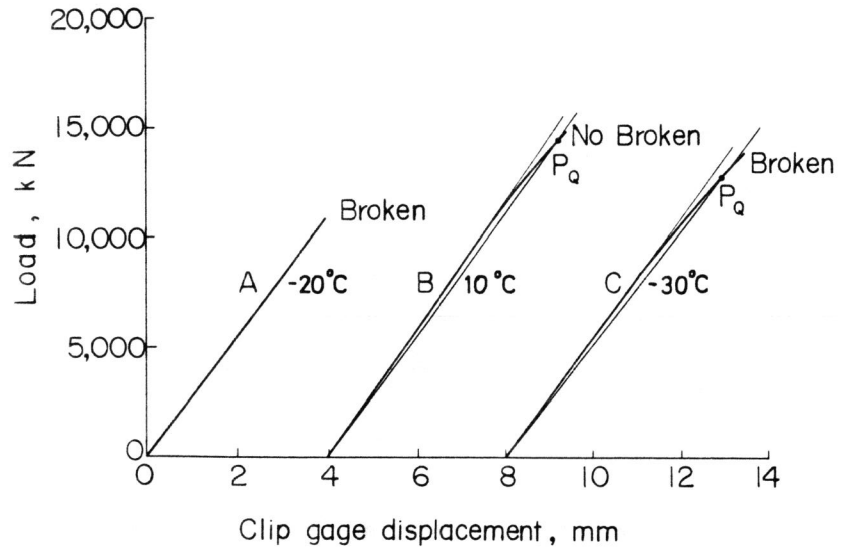


Figure 7 Load-displacement records of 14 RCT tests

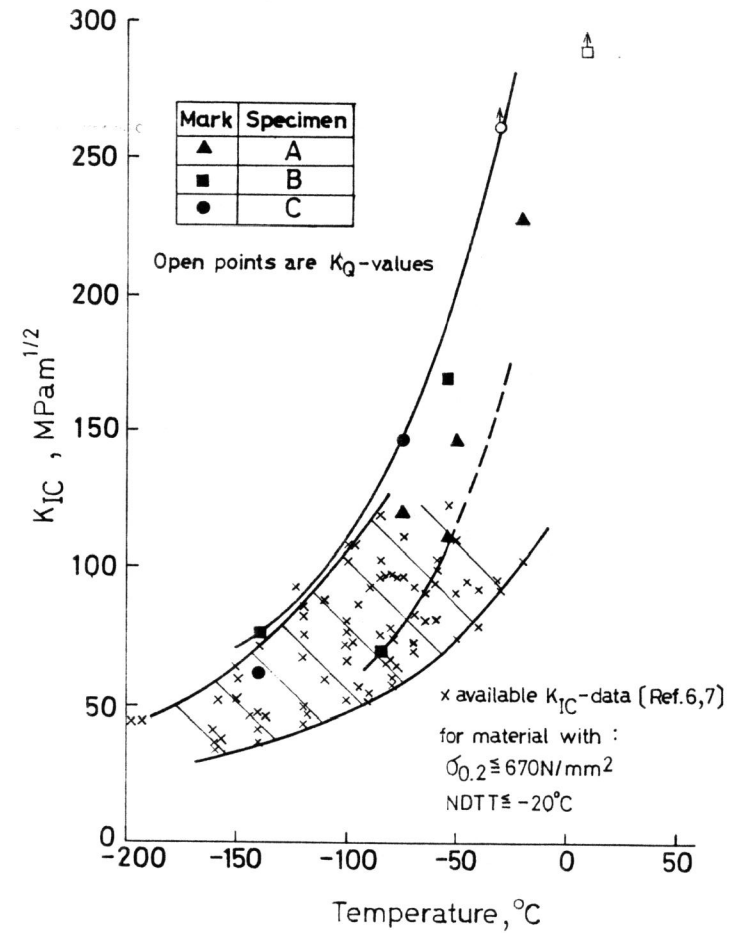


Figure 8 Fracture toughness  $K_{IC}$  of 2.8Ni-Cr-Mo-V steel for rotor forgings